

Specific heat of underdoped cuprate superconductors from a phenomenological layered Boson-Fermion model

P. Salas, M. Fortes, M. A. Solís, and F. J. Sevilla

*Instituto de Física, Apartado postal 20-364,
Universidad Nacional Autónoma de México,
01000 México, D.F., MEXICO*

(Dated: March 6, 2022)

We adapt the Boson-Fermion superconductivity model to include layered systems such as underdoped cuprate superconductors. These systems are represented by an infinite layered structure containing a mixture of paired and unpaired fermions. The former, which stand for the superconducting carriers, are considered as noninteracting zero spin composite-bosons with a linear energy-momentum dispersion relation in the CuO_2 planes where superconduction is predominant, coexisting with the unpaired fermions in a pattern of stacked slabs. The inter-slab, penetrable, infinite planes are generated by a Dirac comb potential, while paired and unpaired electrons (or holes) are free to move parallel to the planes. Composite-bosons condense at a critical temperature at which they exhibit a jump in their specific heat. These two values are assumed to be equal to the superconducting critical temperature T_c and the specific heat jump reported for $\text{YBa}_2\text{Cu}_3\text{O}_{6.80}$ to fix our model parameters namely, the plane impenetrability and the fraction of superconducting charge carriers. We then calculate the isochoric and isobaric electronic specific heats for temperatures lower than T_c of both, the composite-bosons and the unpaired fermions, which matches recent experimental curves. From the latter, we extract the linear coefficient (γ_n) at T_c , as well as the quadratic (αT^2) term for low temperatures. We also calculate the lattice specific heat from the ARPES phonon spectrum, and add it to the electronic part, reproducing the experimental total specific heat at and below T_c within a 5% error range, from which the cubic (βT^3) term for low temperatures is obtained. In addition, we show that this model reproduces the cuprates mass anisotropies.

PACS numbers: 74.20.-z, 74.25.-q, 74.72.kf

I. INTRODUCTION

Since the discovery of cuprate High Temperature Superconductors (HTSC)[1] in 1986 there has been an extraordinary theoretical effort to explain the nature of their microscopic behavior as they are not completely described by the BCS theory [2]. However, very few of these theories consider comparison with specific heat data (or other thermodynamic properties). The HTSC cuprates were the most frequently studied both experimentally and theoretically until Fe based superconductors showed up [3–5]. More recently, the appearance of H_2S at high pressures [6, 7] beat down the record of higher T_c held by the cuprates. But, as can be seen in the many publications related to these newer materials (Fe-based and H_2S), the scenario has become even more entangled.

High T_c cuprate superconductors have peculiarities which represent a benchmark in our current understanding of superconductivity. It is widely accepted that the Cooper pairs, which are responsible for the superconductivity, move in the copper oxide planes resembling a quasi-2D layered system [8], and have coherence lengths much smaller than those in conventional superconductors. The phase diagram [9] of the $\text{YBa}_2\text{Cu}_3\text{O}_x$ shows a dome in the superconducting temperature as a function of the oxygen content x , either by introducing electrons or holes, giving the latter ones the higher temperatures. Cooper pairs are pre-formed at a particular temperature $T^* > T_c$ (pseudogap temperature) above the superconducting dome in the underdoped region [9, 10] (where T_c is smaller than the higher T_c possible), and they undergo a Bose-Einstein Condensation (BEC) as temperature is lowered [11, 12]. There are many other characteristics, but of special interest to us are some recently reported experimental results: the modification of the size of the lattice with oxygen doping [13]; the notorious increase of the superconducting gap magnitude [14] and the dramatic drop of the Fermi temperature T_F when doping is diminished [15]. These features are of crucial importance in our results.

Experiments, reveal four key characteristics of specific heat as a function of temperature: a linear term γ_n in the electronic component, which is believed to come from the normal state electronic specific heat C_{en} above T_c (see Ref. [16] and references therein), and its superconducting counterpart that evolves as γ_0 when the temperature approaches zero. Secondly, there is a quadratic αT^2 term for zero magnetic field [17–19] below T_c (not exhibited in conventional superconductors), which changes to a $H^{1/2}T$ component in the presence of an external magnetic field [20] H , attributable to the superconducting part of the electronic specific heat C_{es} . The reported values for this two constants depend strongly on the conditions of each experiment [17] and on the theoretical method used to relate the different parts of the total specific heat. Thirdly, there is a “jump” in the constant pressure specific heat [21] C_p at T_c (at zero magnetic field and evolving into a “peak” at finite magnetic field), $\Delta C_p/T_c$, attributable to the C_{es} component, indicating a second order phase transition which in turn becomes a smooth maximum as doping decreases [22]. Finally, as the “upturn” in the specific heat at very low temperatures is suppressed, a cubic term βT^3 is also observed [23].

The lattice specific heat C_l of a cuprate, which is generally considered as not changing with the onset of superconductivity [17], turns out to give a crucial contribution to the total specific heat. Although a series of indirect methods have been used to extract the electronic component of the total specific heat [16, 18, 19, 24], we use the Phonon Density of States (PDOS) directly derived from Angle Resolved Photoemission Spectroscopy (ARPES) experiments to calculate the lattice specific heat as shown in Refs. [10] and [25]. We obtain that the electronic specific heat contributes less than 2% to the total.

In the framework of the most basic Boson-Fermion model of superconductivity [11, 26–28], we assume that Cooper pairs are composite-spin-zero-bosons with either zero or nonzero center-of-mass momenta (CMM), coexisting with a fermion fluid of the unpaired electrons. To include the effect of the layered structure of cuprates in the Boson-Fermion model, we calculate the BEC critical temperature and the thermodynamic properties for a system of non-interacting bosons immersed in a periodic multilayer array [29, 30], simulated by an external Dirac comb potential along the perpendicular direction of the CuO_2 planes, while the Cooper pairs are allowed to move freely within the planes, with a linear energy-momentum dispersion relation [28]. The fermion counterpart is treated in a similar way [31] as the boson gas, subject to the same external potential. In this model, we assume that only a small fraction f of the initial N fermions available for pairing participate in the superconductivity at temperature $T = T_c$ and below, where the number of preformed pairs is large enough to achieve coherence independently of the mechanism by which the pairs are formed. This latter assumption is based on the analysis of Uemura’s plot (Fig. 2 of Ref [32]) that shows that critical temperatures for cuprates are in the empirical range [33] of $T_c \approx (0.01 - 0.06)T_F$. However, we are aware that the number of pairs could increase as the temperature is lowered below T_c , but not so much as to drastically modify the final results. At this stage we assume that the number of pairs remains constant.

This paper is organized as follows. In Sec. II we lay out the model from which we derive all the thermodynamic properties for the mixture of composite-boson gas coexisting but non-interacting with the unpaired fermion gas immersed in the layered system. This model depends on two physical parameters: the impenetrability P_0 of the planes, which is responsible for the mass anisotropy M/m observed in the cuprates, and the fraction f of superconducting carriers able to condense.

The expressions for the isobaric electronic specific heat, i.e., the superconducting C_{pes} from the Cooper pairs and the normal C_{pen} from the unpaired fermions are derived in Sec. III. The model parameters are unambiguously determined by the phenomenological properties of $\text{YBa}_2\text{Cu}_3\text{O}_{6.80}$, namely the experimental T_c and the magnitude of jump $\Delta C_p/T_c$, from which the observed T^2 behavior at low temperatures of C_{pes} and the linear dependence on T of C_{pen} are directly obtained. Furthermore, we combine $C_{pes} + C_{pen}$ to show that the total electronic specific heat coincides with the experimental results [25]. Our electronic specific heat constants, $\gamma_n(T_c)$ and α are found to be of the same order of magnitude as the experimental values [34, 35].

In Sec. IV we calculate the specific heat for the lattice C_l using the phonon spectrum obtained by ARPES experiments, and compare it to the one obtained using the PDOS from inelastic neutron scattering (INS) experiments [36, 37]. At the end, we add these three specific heat contributions, $C_{pes} + C_{pen} + C_l \equiv C_p^T$, and compare the result with raw data from the experiments. From C_p^T the cubic coefficient β for low temperatures is extracted giving an excellent agreement with experiments [17, 23, 35].

As a bonus, this model allows us to directly relate the plane impenetrability to the mass anisotropy observed in the HTSC cuprates. This is derived in Sec. V, giving a prediction for M/m consistent with the values reported by experiments [38–40]. Finally, in Sec. VI we present our conclusions.

II. LAYERED STRUCTURE OF UNDERDOPED $\text{YBa}_2\text{Cu}_3\text{O}_x$ CUPRATES

We consider N electrons (or holes) of mass m_e confined in a periodic layered array along the z -direction, which mimics the crystallographic structure of the cuprates, and free to move in the other two directions. The electrons interact via a BCS-type potential, such that when their energies lie within a shell of width $2\hbar\omega_D$ around the Fermi energy E_F of the system, where $\hbar\omega_D$ is the Debye energy, the electrons are able to form *pairs* in momentum space, but only a fraction f of them will become pairs, leaving a set of *pairable but unpaired* electrons. In addition, there are *non-pairable* electrons outside this shell. Based on this model, we will group the N electrons in two major components: Cooper-pairs (boson gas) formed by a fraction f of half the total N electrons inside the pairing shell, and a group of $(1 - f)$ electrons (fermion gas) consisting of the pairable plus the unpairable electrons [11].

A. Composite-bosons: Cooper pairs

We assume the boson-fermion model where the bosons are Cooper-like pairs that appear as resonances in two electrons or two holes as proposed by Friedberg and Lee [26, 27]. In our model, there are $N_B = fN/2$ composite-bosons of mass $m = 2m_e$. The Hamiltonian is

$$H = \sum_{\mathbf{k},s} \varepsilon_{\mathbf{k}} a_{\mathbf{k},s}^\dagger a_{\mathbf{k},s} + \sum_{\mathbf{K}} \varepsilon_{\mathbf{K}} b_{\mathbf{K}}^\dagger b_{\mathbf{K}} + H_1, \quad (1)$$

where $a_{\mathbf{k},s}^\dagger$ and $b_{\mathbf{K}}^\dagger$ are fermion and composite-boson creation operators, respectively, s is the spin and

$$H_1 = \frac{G}{\sqrt{L^3}} [a_{\mathbf{K}/2+\mathbf{k},s} a_{\mathbf{K}/2-\mathbf{k},s} b_{\mathbf{K}}^\dagger v(k) + h.c.] \quad (2)$$

is the interaction Hamiltonian that creates/destroys composite bosons from/into two fermions. Here, $\mathbf{K} = (K_x, K_y, K_z) \equiv \mathbf{k}_1 + \mathbf{k}_2$ is the CMM of the pair, $\mathbf{k} \equiv (\mathbf{k}_1 - \mathbf{k}_2)/2$ is the relative momentum, \mathbf{k}_1 and \mathbf{k}_2 the wave vectors of each electron of the pair, and L^3 is the volume. The form factor $v(k)$ is normalized such that $v(0) = 1$, which defines the coupling constant G . In our model, we assume the zeroth-order approximation [26, 27] so that we keep a mixture of two independent particle systems in a layered structure. The solutions of the Schrödinger equation associated to the Hamiltonian (1), without the H_1 term, may be separated in the $x - y$ and z -directions, so that the energy for each boson particle is $\varepsilon_K = \varepsilon_{K_{x,y}} + \varepsilon_{K_z}$, where $\varepsilon_{K_{x,y}} \equiv 2E_F - \Delta_K$ is the energy of the pair in the $a - b$ crystallographic plane, with Δ_K the temperature independent binding energy.

For $\mathbf{K} \neq 0$, the energy from the Cooper equation may be expanded in a series of powers [28] where the linear term predominates

$$\varepsilon_{K_{x,y}} = \mathbf{e}_0 + C_1(K_x^2 + K_y^2)^{1/2}, \quad (3)$$

with $\mathbf{e}_0 \equiv 2E_F - \Delta_0$ a constant depending on the BCS energy gap $\Delta_0 = 2\hbar\omega_D \exp(-1/\lambda)$ at $\mathbf{K} = 0$ and $T = 0$, $C_1 = (2/\pi)\hbar v_{F2D}$ is the linear term coefficient in 2D, v_{F2D} is the Fermi velocity also in 2D, $\lambda \equiv g(E_F)V$ is the

dimensionless coupling constant in terms of the electronic density of states at the Fermi sea $g(E_F)$ and V , the non-local interaction between fermions.

Along the z -direction we use the Kronig-Penney potential in the Dirac delta limit, following the scheme we previously developed for a boson gas inside a layered structure [29, 30]. The energies are implicitly obtained from the transcendental equation

$$P_0(a/\lambda_0) \sin(\alpha_{K_z} a)/\alpha_{K_z} a + \cos(\alpha_{K_z} a) = \cos(K_z a), \quad (4)$$

with $\alpha_{K_z}^2 \equiv 2m\varepsilon_{K_z}/\hbar^2$ and $P_0 = m\Lambda\lambda_0/\hbar^2$ is a dimensionless parameter which is a measure of the *plane impenetrability*. The constant $\lambda_0 \equiv h/\sqrt{2\pi mk_B T_0}$ is the de Broglie thermal wavelength of an ideal boson gas in an infinite box at the BEC critical temperature $T_0 = 2\pi\hbar^2 n_B^{2/3}/mk_B \zeta(3/2)^{2/3} \simeq 3.31\hbar^2 n_B^{2/3}/mk_B$, with $n_B \equiv N_B/(L^3)$ the boson particle number density and Λ is the strength of the delta potentials $\sum_{n_z=-\infty}^{\infty} \Lambda\delta(z - n_z a)$.

The thermodynamic properties of a boson gas can be derived from the grand potential [41]

$$\Omega(T, L^3, \mu) = U - TS - \mu N_B = \Omega_0 + k_B T \sum_{\mathbf{K} \neq 0} \ln\{1 - \exp[-\beta(\varepsilon_0 + C_1(K_x^2 + K_y^2)^{1/2} + \varepsilon_{K_z} - \mu)]\}, \quad (5)$$

where U is the internal energy, S the entropy, μ the boson chemical potential, $\beta \equiv 1/k_B T$, and the first term in the rhs corresponds to the $\mathbf{K} = 0$ ground state contribution $\Omega_0 = k_B T \ln\{1 - \exp[-\beta(\varepsilon_0 + \mathbf{e}_0 - \mu)]\}$, with $\varepsilon_0 \equiv \hbar^2 \alpha_0^2/2m$ the solution of Ec. (4) for the ground state energy.

Expanding the logarithmic function, substituting sums by integrals in the thermodynamic limit, and evaluating the x, y integrals one obtains

$$\Omega(T, L^3, \mu) = k_B T \ln\{1 - \exp[-\beta(\varepsilon_0 + \mathbf{e}_0 - \mu)]\} - \frac{L^3}{(2\pi)^2} \frac{\Gamma(2)}{C_1^2} \frac{1}{\beta^3} \int_{-\infty}^{\infty} dK_z \mathbf{g}_3(z_b), \quad (6)$$

where we have used the Bose functions [41] $\mathbf{g}_\sigma(t) \equiv \sum_{l=1}^{\infty} t^l/l^\sigma$ and defined $z_b \equiv \exp[-\beta(\varepsilon_{K_z} + \mathbf{e}_0 - \mu)]$.

B. Normal state electrons

The unpaired electrons have the grand potential for an ideal Fermi gas immersed in a layered structure [31]

$$\Omega(T, L^3, \mu_F) = -k_B T \sum_{k=0} \ln\{1 + \exp[-\beta(\varepsilon_k - \mu_F)]\}, \quad (7)$$

where μ_F is the chemical potential of the electron gas and $\varepsilon_k = \hbar^2 k_x^2/2m_e + \hbar^2 k_y^2/2m_e + \varepsilon_{k_z}$ is the energy of each electron free in the $x - y$ directions and constrained by the permeable planes in z -direction. As we did in the case of the boson gas, the energy ε_{k_z} comes from the KP Eq. (4), where we replace K_z by k_z and $P_{0F} = P_0/2$. Converting sums to integrals and evaluating the x, y integrals we have

$$\Omega(T, L^3, \mu_F) = -2 \frac{L^3}{(2\pi)^2} \frac{m_e}{\hbar^2} \frac{1}{\beta^2} \int_{-\infty}^{\infty} dk_z \mathbf{f}_2(z_e), \quad (8)$$

where we use of the Fermi-Dirac functions [41] $\mathbf{f}_\sigma(t) \equiv \sum_{l=1}^{\infty} (-1)^{l-1} t^l/l^\sigma$ and $z_e \equiv \exp[-\beta(\varepsilon_{k_z} - \mu_F)]$. From Eq. (8) each thermodynamic property for the fermion gas may be derived.

C. Critical temperature

The critical temperature of the cuprate is extracted from the bosonic particle number derived from the grand potential, Eq. (6), namely

$$N_B = \frac{1}{\exp\{\beta(\varepsilon_0 + \mathbf{e}_0 - \mu)\} - 1} + \frac{L^3}{(2\pi)^2} \frac{1}{C_1^2 \beta^2} \int_{-\infty}^{\infty} dK_z \mathbf{g}_2(z_b), \quad (9)$$

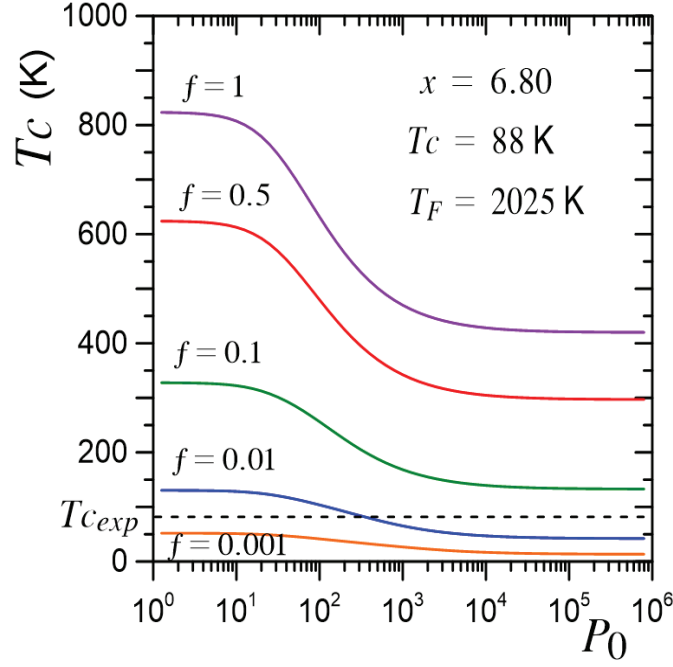


FIG. 1. (Color online) Critical temperature as a function of P_0 for different values of the fraction f of pairable fermions. Dashed line is the experimental $T_c = 88$ K for $\text{YBa}_2\text{Cu}_3\text{O}_{6.80}$ from Ref. [13].

where the first term on the rhs is the order parameter, i.e., the number N_{B0} of particles in the condensed state and the second term is the number of particles in the excited states.

Setting $T = T_c$ in Eq. (9) and taking the chemical potential $\mu_0 = \varepsilon_0 + \mathbf{e}_0$ which corresponds to the ground state, so $N_{B0}(T_c)/N_B \simeq 0$, we have

$$N_B = \frac{L^3}{(2\pi)^2} \frac{1}{C_1^2 \beta^2} \int_{-\infty}^{\infty} dK_z g_2 \{ \exp[-\beta(\varepsilon_{K_z} - \varepsilon_0)] \}, \quad (10)$$

which must be solved numerically using the fact that in the $\text{YBa}_2\text{Cu}_3\text{O}_x$ systems there are two copper-oxide regions per unit cell where superconductivity takes place, so the parameter a is fixed to half the crystallographic constant c .

Here we point out the following fact: from the relation of the Fermi energy in terms of the superconducting carrier density [41], $E_F = \hbar^2(3\pi^2)^{2/3}n_s^{2/3}/2m$, for $\text{YBa}_2\text{Cu}_3\text{O}_{6.80}$ with $T_F = 2025$ K obtained by extrapolation of the T_F curve of Fig. 4 of Ref. [15], we obtain the carrier density as $n_s = 9.37 \times 10^{26}/\text{m}^3$. On the other hand, the BEC critical temperature for an ideal Bose gas created from a fermion gas where all fermions are paired [42], is $T_0 = 0.218T_F$ with T_F the Fermi temperature of the original Fermi gas, so T_0 gives 441.5 K for this particular superconductor. Introducing this value in the definition of T_0 given in Sec. II A, one has $n_B = 1.658 \times 10^{26}/\text{m}^3$ for the boson density number, which is almost an order of magnitude smaller than the n_s calculated above. However, as we mentioned before, by analyzing the Uemura data in Fig. 2 of Ref. [32] and localizing the diagonal lines labeled as $T = T_F$ and $T = T_0$ (labeled as T_B), one would expect that the actual number of superconducting carriers for the cuprates (which we will call n_b) would be about two orders of magnitude smaller than the n_s calculated above. Therefore, we assume that only a fraction f of the maximum possible value n_B is participating in the boson gas responsible for the superconductivity, hence $n_b = fn_B$, and we expect this fraction to be $f < 0.01$, as shown in Fig. 1, consistent with the analysis of Refs. [17] and [33].

Therefore, the BEC critical temperature for a fraction f of N_B bosons is

$$T_{0f} = \frac{2\pi\hbar^2 n_B^{2/3}}{mk_B \zeta(3/2)^{2/3}} = T_0 f^{2/3}, \quad (11)$$

the quotient of the fraction of an ideal gas BEC temperature in terms of its T_F is

$$\frac{T_{0f}}{T_F} = \frac{2\pi f^{2/3}}{(6\pi^2)^{2/3} \zeta(3/2)^{2/3}} = 0.218 f^{2/3}, \quad (12)$$

and the thermal wavelength is $\lambda_{0f} = h/\sqrt{2\pi m k_B T_{0f}} = \lambda_0/f^{1/3}$. For $f = 1$ we recover the case where all pairable fermions participate in the boson gas.

Additional experimental parameters of $\text{YBa}_2\text{Cu}_3\text{O}_{6.80}$ that we use in our calculations are: the critical temperature [13] $T_{cexp} = 88$ K; the superconducting parameter [14] $\Delta_0 = 50$ meV; the crystallographic [13] $c = 11.71$ Å, giving $a = c/2 = 5.855$ Å and $a/\lambda_0 = 0.233$. Finally, we take the height of the jump $\Delta C/T_c \simeq 20$ mJ/mol K² from the data published in Ref. [35]. In addition, we use the relation for the Fermi energy $E_{F3D} = [(3\pi^2)^{2/3}/2\pi]E_{F2D}$ for a 3D system in terms of the Fermi energy for a 2D system $E_{F2D} = \frac{1}{2}m_e v_{F2D}^2$.

In Fig. 1 we show the critical temperature as a function of the parameter P_0 for several values of f . The dashed line represents the experimental critical temperature for $\text{YBa}_2\text{Cu}_3\text{O}_{6.80}$. As can be seen from this figure, there is only a narrow interval of values of $f \in [0.005, 0.05]$, that fits the experimental condition [35] $T_c = 88$ K, which in turn determines a set of values of P_0 . This is consistent with our previous assumption that only a small percentage of the initially pairable fermions actually form pairs. In order to narrow down the range of both values, we obtain the magnitude of the jump in the electronic specific heat from experiments as shown in the next section.

III. ELECTRONIC SPECIFIC HEAT

The cuprate total electronic specific heat at constant pressure C_{pe} is the specific heat of the gas of Cooper-pairs plus the specific heat of the gas of electrons, $C_{pe} = C_{pes} + C_{pen}$, each of which is calculated in this section.

A. Superconducting electronic specific heat

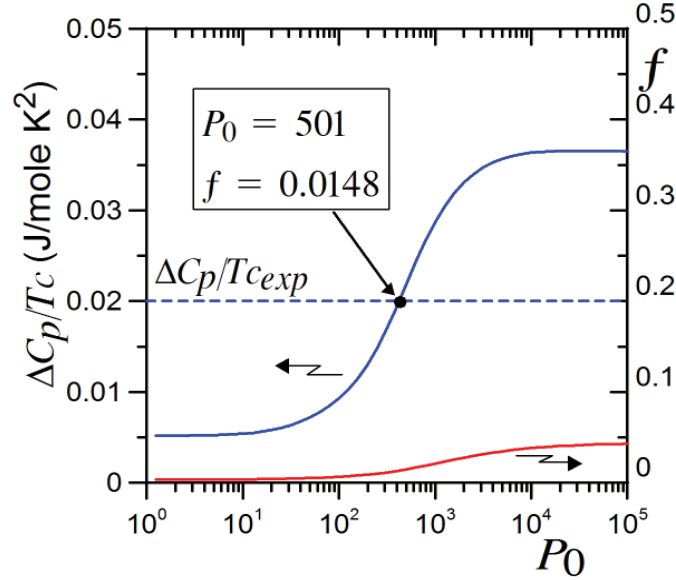


FIG. 2. (Color online) Jump height of the specific heat and f as a function of P_0 . Dashed line is the experimental $\Delta C_p/T_c = 20$ mJ/mole K² from Ref. [35].

The superconducting electronic specific heat at constant volume C_{Ves} for the Cooper pairs gas is $C_{Ves} = [T \frac{\partial S}{\partial T}]_{N,L^3}$. Hence, taking the fraction f , we have

$$\begin{aligned} \frac{C_{Ves}}{N_B k_B} = & \frac{L^3}{f N_B (2\pi)^2 C_1^2} \left[\frac{2}{\beta} \int_{-\infty}^{\infty} adK_z g_2(z_b) \left[2\varepsilon_{K_z} - \varepsilon_0 + \mathbf{e}_0 - \mu + T \frac{d\mu}{dT} \right] - \right. \\ & \left. \int_{-\infty}^{\infty} adK_z (\varepsilon_{K_z} - \varepsilon_0) \ln\{1 - z_b\} \left[\varepsilon_{K_z} + \mathbf{e}_0 - \mu + T \frac{d\mu}{dT} \right] + \frac{6}{\beta^2} \int_{-\infty}^{\infty} adK_z g_3(z_b) \right], \end{aligned} \quad (13)$$

where μ and its derivative are implicitly obtained from the number equation for $T \geq T_c$

$$N_B = \frac{L^3}{(2\pi)^2} \frac{\Gamma(2)}{C_1^2} \frac{1}{\beta^2} \int_{-\infty}^{\infty} dK_z \mathbf{g}_2(z_b). \quad (14)$$

The corresponding specific heat at constant pressure is derived from the relation $C_{pes} = C_{Ves} + TL^3 \kappa_T \left[\frac{\partial P}{\partial T} \right]_{N,L^3}^2$, with κ_T the isothermal compressibility. After some algebra, we find

$$\frac{C_{pes}}{N_B k_B} = \frac{C_{Ves}}{N_B k_B} - \left(\frac{\int_{-\infty}^{\infty} dK_z \ln\{1 - z_b\}}{\int_{-\infty}^{\infty} dK_z \mathbf{g}_2(z_b)} \right) \left[\frac{L^3}{f(2\pi)^2} \frac{1}{C_1^2 \beta^2} \left(3 \int_{-\infty}^{\infty} dK_z \mathbf{g}_3(z_b) + \beta \int_{-\infty}^{\infty} dK_z \mathbf{g}_2(z_b) \right) \right]^2. \quad (15)$$

In Fig. 2 we show the magnitude of the height of the difference between the constant pressure specific heat above and below T_c divided by T_c , $\Delta C_{pes}/T_c$, as a function of P_0 together with the fraction of Cooper-pairs f . The horizontal dashed line represents the experimental result [35] $|\Delta C_{pes}/T_c|_{exp} = 20$ mJ/mole K², and the points where the curves cross this line are the values of $P_0 = 501$ and $f = 0.0148$ that fulfill the conditions for YBa₂Cu₃O_{6.80}. With these two parameters we are able to calculate all the thermodynamic properties for $T \leq T_c$.

B. Normal electronic specific heat

The specific heat at constant volume of the unpaired electrons is obtained from Eq. (8)

$$\begin{aligned} \frac{C_{Ven}}{N k_B} &= \frac{1}{(1-f)} \frac{L^3}{N(2\pi)^2} \frac{m_e}{\hbar^2} \left[\frac{1}{\beta} \int_{-\infty}^{\infty} dk_z \mathbf{f}_2(z_e) \right. \\ &\quad \left. + 2 \int_{-\infty}^{\infty} dk_z \ln\{1 + z_e\} \left[2\varepsilon_{k_z} - \mu_F + T \frac{d\mu_F}{dT} \right] + 2 \int_{-\infty}^{\infty} dk_z \frac{\varepsilon_{k_z} \{ \varepsilon_{k_z} - \mu_F + T \frac{d\mu_F}{dT} \}}{\exp[\beta(\varepsilon_{k_z} - \mu_F)] + 1} \right]. \end{aligned} \quad (16)$$

Again, the chemical potential μ_F and its derivative are extracted from the corresponding number equation

$$N = \frac{1}{(1-f)} \frac{2L^3}{(2\pi)^2} \frac{m_e}{\hbar^2} \frac{1}{\beta} \int_{-\infty}^{\infty} dk_z \ln\{1 + z_e\}. \quad (17)$$

Using the relation for the specific heat at constant pressure, we finally obtain

$$\begin{aligned} \frac{C_{pen}}{N k_B} &= \frac{C_{Ven}}{N k_B} + \frac{2L^3}{(1-f)N(2\pi)^2} \frac{m_e}{\hbar^2} \beta \left(\frac{\int_{-\infty}^{\infty} \frac{dk_z}{\exp[\beta(\varepsilon_{k_z} - \mu_F)] + 1}}{\left(\int_{-\infty}^{\infty} dk_z \ln\{1 + z_e\} \right)^2} \right) \\ &\quad \times \left[\int_{-\infty}^{\infty} dk_z \ln\{1 + z_e\} \left[\varepsilon_{k_z} - \mu_F + T \frac{d\mu_F}{dT} \right] + \frac{2}{\beta} \int_{-\infty}^{\infty} dk_z \mathbf{f}_2(z_e) \right]^2. \end{aligned} \quad (18)$$

C. Total electronic specific heat

In Fig.3 we show the total C_{pe} (continuous line), together with the Cooper-pairs (dash-dot line) and fermions (dashed line) specific heats. We include two experimental curves for YBa₂Cu₃O_{6.70} (triangles) and YBa₂Cu₃O_{6.90} (diamonds) from Fig. 5 of Ref. [25], where the authors present exclusively the electronic part after successfully extracting the phonon contribution.

We obtain the parameter $\gamma_n(T_c) \equiv C_{pen}(T_c)/T_c = 45$ mJ/mol K² from the linear behavior of the normal electronic specific heat calculated data and the quadratic term coefficient from the superconducting electronic specific heat $\alpha = 0.038$ mJ/mol K³, which comes from the Cooper pairs. Experimental data for $\gamma_n(T_c)$ yields, for example, 32 mJ/mol K² for $x = 0.95$ from Ref. [34], while for α we find 0.064 mJ/mol K³ for $x = 0.80$ from Ref. [35], both in the same order of magnitude as our results.

There is a *non-zero* value for γ_0 , at $T = 0$, as stated in Refs. [16, 43, and 44] for oxygen content $x > 0.6$, which is different from the extrapolation of $\gamma_n(T_c)$ when $T \rightarrow 0$, suggesting that the pairing mechanism continues to take place. However, in our model we are unable to determine γ_0 because we do not include the rate at which pairs continue

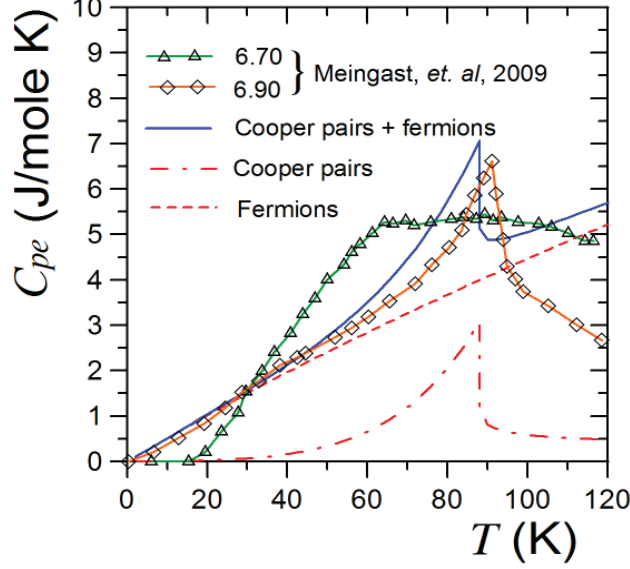


FIG. 3. (Color online) The Cooper pair and the fermionic contributions to constant pressure electronic specific heat for $\text{YBa}_2\text{Cu}_3\text{O}_{6.80}$, using $P_0 = 501$ and $f = 0.0148$, compared to the experimental data of Meingast, *et. al.* for two different doping values [25].

to form for temperatures below T_c towards $T = 0$. Furthermore, above T_c paired fermions may decouple through complex mechanisms that we have not considered in this analysis.

Other thermodynamic properties, such as the entropy as well as the Helmholtz free energy of the boson-fermion mixture inside a layered system will be published elsewhere.

IV. TOTAL SPECIFIC HEAT

The total specific heat of $\text{YBa}_2\text{Cu}_3\text{O}_{6.80}$ is the electronic plus the lattice specific heat, i.e., $C_p^T = C_l + C_{pes} + C_{pen}$. In this section we obtain the lattice specific heat C_l and add it to the electronic contribution, showing that our resulting curves for C_p^T and C_p^T/T lie very close to the raw data reported by some experiments.

A. Lattice specific heat

The total internal energy of a crystal is given by [45]

$$U = \int \frac{\hbar\omega G(\omega)d\omega}{(\exp[\hbar\omega/k_B T] - 1)}, \quad (19)$$

where ω is the vibrational mode frequency, $G(\omega)$ is the PDOS and $\hbar\omega$ is the energy of each mode. The constant volume specific heat for the lattice is then given by

$$C_{Vl} = k_B \int \frac{(\hbar\omega/k_B T)^2 \exp[\hbar\omega/k_B T] G(\omega)d\omega}{(\exp[\hbar\omega/k_B T] - 1)^2}. \quad (20)$$

We use a phenomenological procedure to calculate the lattice specific heat of the layered cuprate. Specifically, we take the experimental results for the PDOS and introduce it in the theoretical expressions given above. We analyze the results of three different experiments: two from INS[36, 37], while the third one is based on a more recent ARPES technique [25].

Although our lattice specific heat has been calculated at constant volume, a simple calculation of the difference between $C_{pl} - C_{Vl} = TBV_{mol}\tau^2$ shows that it is smaller than 1 Joule/mol K at $T = T_c$, where τ is the volumetric

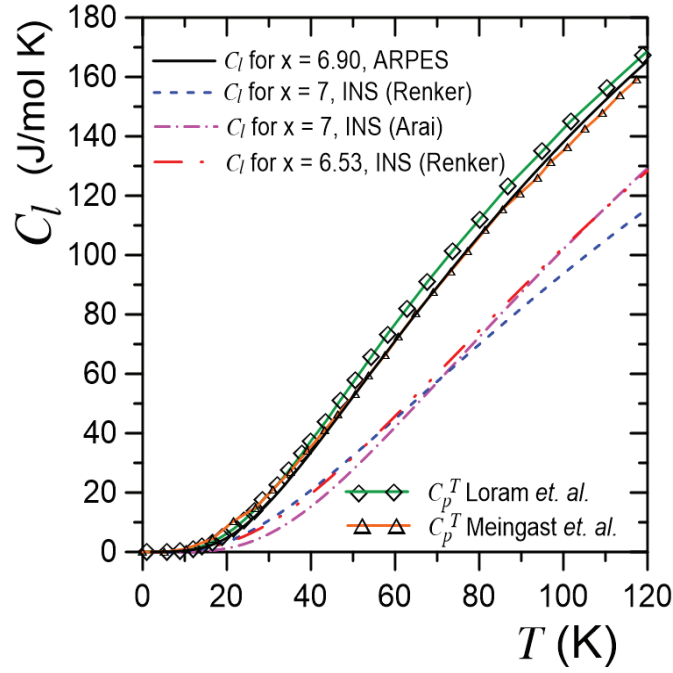


FIG. 4. (Color online) Lattice specific heat for different doping values obtained using Eq. 20 together with the experimental total specific heat from Refs. [25] and [48].

thermal expansion coefficient taken from Ref. [46], B is the bulk modulus from Ref. [47] and V_{mol} is the molar volume. Note that this approach already takes into account the anharmonic terms in the lattice component, at least up to the temperature interval considered. Therefore we will refer to the lattice specific heat using only the l subindex.

We obtain the results drawn in Fig. 4 by using the PDOS from the INS data for $\text{YBa}_2\text{Cu}_3\text{O}_x$ with $x = 7$ (short dash line) and $x = 6.53$ (dash-dot-dot line) from the curves of Ref. [36], and for $x = 7$ from [37] (dash-dot line), and introduce each one in Eq. (20) to perform the integrals numerically. The difference between the first two curves and the third one is small in the $20 \text{ K} < T < 80 \text{ K}$ interval and for $T > 80 \text{ K}$ it widens progressively. In the same Fig. 4, we plot our calculation of the lattice specific heat (solid line) using the results from ARPES[25] for $x = 7$ together with the curves adapted for the total “raw data” experimental specific heat for $x = 6.67$ from Ref. [48] (diamonds) and for $x = 6.70$ from Ref. [25] (triangles). We find that our calculated C_l (solid line) using the ARPES density of state is close to the experimental total specific heat C_p^T , however, there is a significant difference using INS data (around the 30 %).

Three remarks are in order: first, the difference between the lattice specific heat using ARPES and INS around the transition point T_c is at least 30% (it diminishes as T lowers), which shows that the use of the latter is somehow obsolete and should be discarded, as stated in Ref. [10]. Second, the difference in the lattice specific heat between two near doping values is in general small, and allows us to safely use the $x = 7$ PDOS from ARPES for other dopings, such as $x = 6.80$. Finally, in the curves of the experimental C_p^T shown in Fig. 4, the jump height is barely noticed, which is another signal that the lattice component is dominant. For completeness, we calculated the lattice specific heat for the $\text{YBa}_2\text{Cu}_3\text{O}_6$ non-superconducting compound using the PDOS from INS (not shown in the graphic) which lies very close to the other doping curves obtained also from INS. Above T_c the lattice specific heat we obtain is still very close to the experimental C_p^T at least for up to $T = 200 \text{ K}$ (not shown).

In summary, the fact that the lattice specific heat C_l and the total experimental specific heat C_p^T are very close leads to the conclusion that the contribution from the electronic components is very small, as will be shown in the next subsection.

B. Total specific heat of $\text{YBa}_2\text{Cu}_3\text{O}_{6.80}$

The total specific heat C_p^T is the sum of all three components: the electronic specific heat we calculated for both composite-bosons and unpaired electrons with the parameters $P_0 = 501$ and $f = 0.0148$, in addition to the lattice

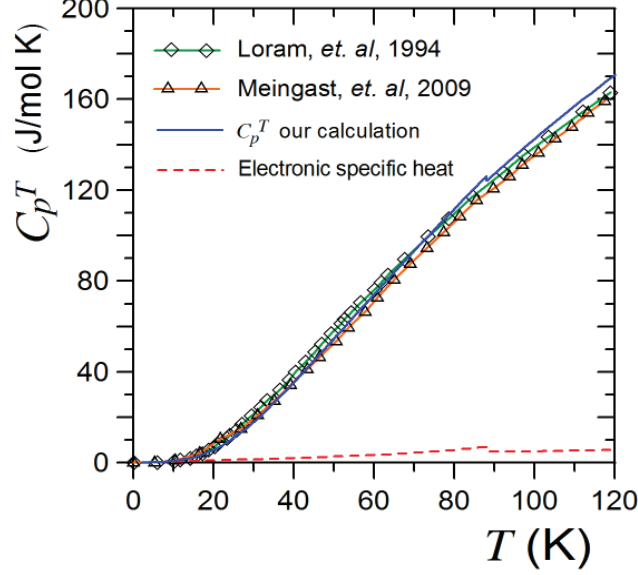


FIG. 5. (Color online) Total calculated constant pressure specific heat with the results from Refs. [25] and [48]. The contribution of the electronic component shown separately.

specific heat from ARPES. In Figs. 5 and 6 we plot the total specific heat together with the electronic part (normal plus superconducting) to emphasize the size of its contribution.

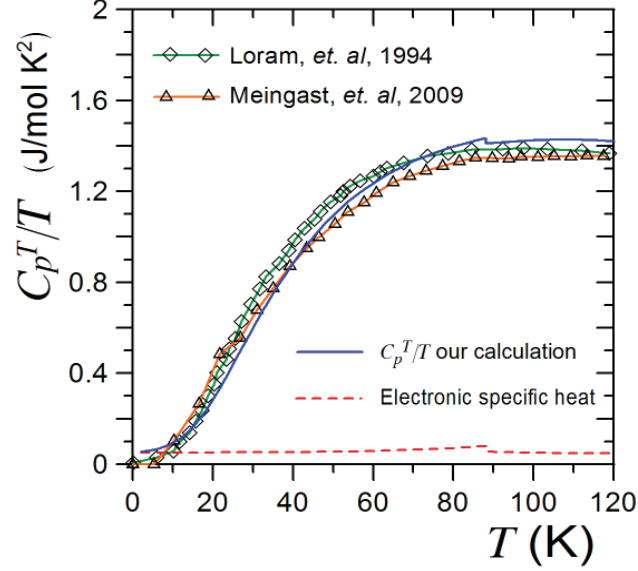


FIG. 6. (Color on line) Total calculated constant pressure specific heat over temperature with the results from Refs. [25] and [48]. The contribution of the electronic component shown separately.

In these figures we observe that the total experimental specific heat curves for both, C_p^T and C_p^T/T , are satisfactorily reproduced by adding the three analyzed components. The minor difference between the experimental shape of the curve and ours for C_p^T/T at and below T_c observed in Fig. 6 may be due to the interactions among the particles and from the dynamical formation of Cooper-pairs for $T < T_c$.

Accordingly, we claim that the contribution of the electronic specific heat to the total is less than the 5%, as suggested in Refs. [25] and [24].

Finally, by plotting our total specific heat C_p^T/T vs T^2 (not shown), we reproduce the βT^3 term observed in experiments [17, 18] for $T < 5$ K. This behavior is expected if the Debye model is used, but it is not trivial for any other lattice model. We find $\beta = 0.362$ mJ/mol K⁴ compared to 0.333 for $x = 6.80$ reported in Ref. [35], 0.305 for $x = 7$ in Ref. [17] and 0.392 for $x = 6.50$ in Ref. [23].

V. MASS ANISOTROPY

Using the equations derived in Sec. II A we can make a direct connection between one of the observed features of cuprate superconductors and our model: the mass anisotropy.

From Eq. (4) we note that when $P_0 \rightarrow 0$, the energy goes to the free-particle energy $\varepsilon_{K_z} \rightarrow \hbar^2 K_z^2/2m$ in the z direction [30]. Also, when the particle energies are small, $\varepsilon_{K_z} < \hbar^2/2ma^2$, one can expand the first term of Eq. (4) around ε_0 , so

$$\varepsilon_{K_z} \cong \varepsilon_0 + \frac{\hbar^2}{Ma^2}(1 - \cos K_z a), \quad (21)$$

where ε_0 satisfies $P_0(a/\lambda_0)\sin(\alpha_0 a)/\alpha_0 a + \cos(\alpha_0 a) = 1$, and M is the effective mass. This last equation is the most commonly used for quasi-bidimensional models of superconductors [49], but it is a model that is constrained only to the first energy band and for zero ground state energy, i.e., $\varepsilon_0 = 0$ when $K_z = 0$, which is not the general case for layered systems [30].

Writing explicitly the effective mass M in Eq. (21) we have

$$M/m = |\sin(\alpha_0 a) - (P_0(a/\lambda_0) + 1)\cos(\alpha_0 a)/(\alpha_0 a)|/(\alpha_0 a). \quad (22)$$

Introducing the values for $P_0, f, a/\lambda_0$ and ε_0 previously obtained we get $M/m = 12.3$. Experimental reports give 5.3 for $x = 7$ from Refs. [39 and 40], 7.0 for $x = 6.92$ from [39] and 10.8 for $x = 6.80$ from [38], showing an increasing value dependence as doping lowers, which sets our result within the expected range.

VI. CONCLUSIONS

While most procedures take the experimental curves of the total specific heat and subtract components, we qualitatively and quantitatively construct the total constant pressure specific heat for the $\text{YBa}_2\text{Cu}_3\text{O}_x$ underdoped cuprates from a simple, first principles model: the Boson-Fermion theory of superconductivity applied to layered systems. The model assumes the Cooper pairs as a composite-boson gas coexisting with an unpaired electrons (or holes) fermion gas. Both gases are constrained in a stacked slabs structure modeled by a Dirac comb potential in the perpendicular direction to the CuO_2 planes. Although no residual interactions among Cooper pairs and unpaired fermions are considered, the model reproduces qualitatively and quantitatively the experimental curves of the electronic part and the total specific heat.

For a specific underdoped cuprate we take the CuO_2 plane separation as our a constant. In addition, we use the experimental critical temperature and the electronic specific heat jump to set our phenomenological parameters: the planes impenetrability P_0 and the fraction f of fermions that turn into Cooper pairs.

The total specific heat is calculated by adding the specific heats coming from the composite-bosons (superconducting electronic specific heat), unpaired fermions (normal electronic specific heat) and the lattice calculated from the ARPES PDOS. The resulting curves for $\text{YBa}_2\text{Cu}_3\text{O}_{6.80}$ are compared to the experimental results, giving a remarkable agreement within a 5% error range for temperatures below T_c .

We derive the linear dependence on temperature $\gamma_n T$ and the quadratic one αT^2 for the electronic specific heat, obtaining $\gamma_n(T_c) = 45$ mJ/mol K² and $\alpha = 0.038$ mJ/mol K³ for $T < T_c$, in agreement with the experimental data reported for similar cuprates, which is an additional check of consistency for our model. We show that the correspondence relating the normal electronic specific heat with the unpaired fermions, and the superconducting term with the Cooper pairs, is a valid assumption. These results make plausible the assumption that not all pairable fermions in the Fermi sea are paired, even at temperatures near zero, and that the jump in the specific heat is a direct consequence of the condensation of the pairs. We also confirm that the lattice specific heat from the phonon density of states by ARPES measurements is better than that obtained from INS experiments. It can also be seen that the calculated total specific heat shows the same temperature cubic behavior for $T < 5$ K as shown experimentally, with a coefficient $\beta = 0.362$ mJ/mol K⁴. Additionally, we find that the electronic specific heat (normal plus superconducting) has a contribution $< 5\%$ of the total at the transition temperature. Finally, another direct outcome is the reproduction of the high mass anisotropy of the cuprates, giving $M/m = 12.3$ for the compound analyzed.

The present method may be applied to other HTSC cuprates and to some iron-based superconductors, which will be done in a future publication.

We acknowledge the partial support from grants PAPIIT IN-111613 and CONACYT 221030.

-
- [1] G. Bednorz and K. A. Müller, Z. Phys. B. **64**, 1175 (1986).
 - [2] J. Bardeen, L. N. Cooper and J. R. Schrieffer, Phys. Rev. **108**, 189 (1957).
 - [3] A. Chubukov and P. J. Hirschfeld, Phys. Today **86**, 46 (2015).
 - [4] D. C. Johnston, Adv. Phys. **59**, 803 (2010).
 - [5] X. Luo and X. Chen. Sci. China Matter. **58**, 77 (2015).
 - [6] A. P. Drozdov, M. I. Erements, I. A. Troyan, V. Ksenofontov and S. I. Shylin, Nature Letters **525**, 73 (2015).
 - [7] J. E. Hirsh and F. Marsiglio, Physica C **511**, 45 (2015).
 - [8] C. P. Poole Jr., H. A. Farach, R. J. Creswick, R. Prozorov, *Superconductivity*, 2nd Ed. (Elsevier, The Netherlands, 2007) p195.
 - [9] A. Shekhter, B. J. Ramshaw, R. Liang, W. N. Hardy, D. A. Bonn, F. F. Balakirev, R. D. McDonald, J. B. Betts, S. C. Riggs and A. Migliori, Nature **498**, 75 (2013).
 - [10] J. R. Cooper, J. W. Loram, I. Kokanovic, J. G. Storey and J. L. Tallon, Phys. Rev. B **89**, 201104 (2014).
 - [11] M. Casas, N. J. Davidson, M. de Llano, T. A. Mamedov, A. Puente, R. M. Quick, A. Rigo, and M. A. Solís, Physica A **295**, 425 (2001).
 - [12] D. M. Eagles, Phys. Rev. **186**, 456 (1969).
 - [13] R. Liang, D. A. Bonn and W. N. Hardy, Phys. Rev. B **73**, 180505 (2006).
 - [14] M. Sutherland, D. G. Hawthorn, R. W. Hill, F. Ronning, S. Wakimoto, H. Zhang, C. Proust, E. Boaknin, C. Lupien, L. Taillefer, R. Liang, D. A. Bonn, W. N. Hardy, R. Gagnon, N. E. Hussey, T. Kimura, M. Nohara and H. Takagi, Phys. Rev. B **67**, 174520 (2003).
 - [15] S. E. Sebastian, N. Harrison, M. M. Altarawneh, C. H. Mielke, R. Liang, D. A. Bonn, W. N. Hardy and G. G. Lonzarich, PNAS **107**, 6175 (2010).
 - [16] R. A. Fisher, J. E. Gordon and N. E. Phillips, *Handbook of High-Temperature Superconductivity, Theory and Experiment*, edited by J. Robert Schrieffer (Springer, New York 2007) p345.
 - [17] Y. Wang, B. Revaz, A. Erb and A. Junod, Phys. Rev. B **63**, 094508 (2001).
 - [18] K. A. Moler, D. L. Sisson, J. S. Urbach, M. R. Beasley, A. Kapitulnik, D. J. Baar, R. Liang and W. N. Hardy, Phys. Rev. B **55**, 3954 (1997).
 - [19] D. A. Wright, J. P. Emerson, B. F. Woodfield, J. E. Gordon, R. A. Fisher and N. E. Phillips, Phys. Rev. Lett **82**, 1550 (1999).
 - [20] G. E. Volovik, JETP Lett **58**, 469 (1993).
 - [21] A. Junod, M. Roulin, J. Y. Genoud, B. Revaz, A. Erb, E. Walker, Physica C **275**, 245 (1997).
 - [22] J. W. Loram, K. A. Mirza, J. R. Cooper and J. L. Tallon, J. Phys. Chem. Solids **59**, 2091 (1998).
 - [23] K. A. Moler, D. J. Baar, J. S. Urbach, R. Liang, W. N. Hardy and A. Kapitulnik, Phys. Rev. Lett **73**, 2744 (1994).
 - [24] J. W. Loram, K. A. Mirza, J. R. Cooper and W. Y. Liang, Phys. Rev. Lett. **71**, 1740 (1993).
 - [25] C. Meingast, A. Inaba, R. Heid, V. Pankoke, K-P Bohnen, W. Reichardt and T. Wolf., J. Phys. Soc. Jap. **78**, 074706 (2009).
 - [26] R. Friedberg and T. D. Lee, Phys. Letters A **138**, 423 (1989); R. Friedberg and T. D. Lee, Phys. Rev. B **40**, 6745 (1989).
 - [27] R. Friedberg, T. D. Lee and H. C. Ren, Phys. Letters A **152**, 417 (1991).
 - [28] S. K. Adhikari, M. Casas, A. Puente, A. Rigo, M. Fortes, M. A. Solís, M. de Llano, A. A. Valladares and O. Rojo, Phys. Rev. B **62**, 8671 (2000).
 - [29] P. Salas, M. Fortes, M. de Llano, F. J. Sevilla, and M. A. Solís, J. of Low Temp. Phys. **159**, 540 (2010).
 - [30] P. Salas, F. J. Sevilla, M. Fortes, M. de Llano, A. Camacho, and M. A. Solís, Phy. Rev. A **82**, 033632 (2010).
 - [31] P. Salas, and M. A. Solís, J. of Low Temp. Phys. **175**, 427 (2014).
 - [32] Y. J. Uemura, Physica B **374**, 1 (2006).
 - [33] S. K. Adhikari, M. Casas, A. Puente, A. Rigo, M. Fortes, M. A. Solís, M. de Llano, A. A. Valladares and O. Rojo, Physica C **341**, 233 (2000).
 - [34] A. Junod, D. Eckert, T. Graf, G. Triscone and J. Muller, Physica C **162**, 1401 (1989).
 - [35] J. P. Emerson, D. A. Wright, B. F. Woodfield, J. E. Gordon, R. A. Fisher and N. E. Phillips, Phys. Rev. Lett. **82**, 1546 (1999).
 - [36] B. Renker, F. Gompf, E. Gering, D. Ewert, H. Rietschel and A. Dianoux, Z. Phys. B **73**, 309 (1988); B. Renker, F. Gompf, E. Gering, G. Roth, W. Reichardt, D. Ewert, H. Rietschel and H. Mutka, Z. Phys. B **71**, 437 (1988).
 - [37] M. Arai, K. Yamada, Y. Hidaka, S. Itoh, Z. A. Bowden, A. D. Taylor and Y. Endoh, Phys. Rev. Lett. **69**, 359 (1992).
 - [38] M. Roulin, A. Junod, and E. Walker, Physica C **296**, 137 (1998).
 - [39] A. Junod, A. Erb and C. Renner, Physica C **317**, 333 (1999).
 - [40] M. Chiao, R. W. Hill, C. Lupien, L. Taillefer, P. Lambert, R. Gagnon and P. Fournier, Phys. Rev. B. **62**, 3554 (2000).
 - [41] R. K. Pathria, *Statistical Mechanics*, 2nd Ed. (Pergamon, Oxford, 1996) p506.
 - [42] F. J. Sevilla, M. Grether, M. Fortes, M. de Llano, O. Rojo, M. A. Solís and A. A. Valladares, J. Low Temp. Phys. **121**,

281 (2000).

- [43] W. Y. Liang, J. W. Loram, K. A. Mirza, N. Athanassopoulou and J. R. Cooper, *Physica C* **263**, 277 (1996).
- [44] C. Uher in *Handbook of Superconductor Materials, Vol. I*, edited by D. A. Cardwell and D. S. Ginley (Institute of Physics Publishing Ltd, Bristol and Philadelphia, 2003) p75.
- [45] Ch. Kittel, *Introduction to Solid State Physics*, 2nd Ed. (John Wiley and Sons, New York, 1965) p116.
- [46] P. Nagel, V. Pasler and C. Meingast, *Phys. Rev. Lett.* **85**, 2376 (2000).
- [47] A. Koblishka-Veneva, N. Sakai, S. Tajima and M. Murakami in *Handbook of Superconductor Materials, Vol. I*, edited by D. A. Cardwell and D. S. Ginley (Institute of Physics Publishing Ltd, Bristol and Philadelphia, 2003) p893.
- [48] J. W. Loram, K. A. Mirza, J. R. Cooper, W. Y. Liang and J. M. Wade, *J. of Sup.* **7**, 243 (1994).
- [49] X-G Wen and R. Kan, *Phys. Rev. B* **37**, 595 (1988).